

# Electron Microscopy of the Tin-oxide Nanolayer Formed on the Surface of Sn-Ag-Cu Alloys

H Sosiati<sup>1</sup>, N Kuwano<sup>2</sup> and S Hata<sup>3</sup>

<sup>1</sup>Department of Mechanical Engineering, Faculty of Engineering, Universitas Muhammadiyah Yogyakarta, Yogyakarta 55183, Indonesia.

<sup>2</sup>Mechanical Precision Engineering, Malaysia-Japan International Institute of Technology (MJIIT), University of Technology Malaysia (UTM) International Campus, Jalan Semarak 54100 Kuala Lumpur, Malaysia.

<sup>3</sup>Interdisciplinary Graduate School of Engineering Sciences, Kyushu University, Kasuga, Fukuoka 816-8580, Japan

E-mail : hsosiati@gmail.com

**Abstract.** Sn-Ag-Cu alloy used in the present study is commercial Sn-3.0Ag-0.5Cu solder ball alloys with a diameter of 400 and 300  $\mu\text{m}$  which were long term atmospheric oxidized for about 6 years (specimen-1) and under high temperature/humidity at 85°C and relative humidity of 85% for 2140 h, respectively. Morphologies and nanostructure of the oxide nanolayers formed on the surface of Sn-Ag-Cu alloys were studied from the interface of the oxide film and the tin substrate by transmission electron microscopy (TEM) to verify the oxidation mechanism. Cross-sectional TEM specimens were prepared using a focused-ion-beam (FIB) micro-sampling technique. Before the FIB fabrication, the specimen surface was coated with carbon (C) and tungsten (W) films. Inhomogeneous thickness of tin-oxide nanolayer formed on specimen-1 and specimen-2 were fluctuated between 20-40 nm and 40-50 nm, respectively. The nanolayer on specimen-1, however, consists of polycrystalline SnO and SnO<sub>2</sub>, whereas the one on the specimen-2 comprises of polycrystalline SnO<sub>2</sub>. High resolution (HRTEM) image and fast Fourier transformation (FFT) spectra corresponding to the interface and the substrate areas have confirmed those results. The results verify that at very long atmospheric oxidation Sn was gradually oxidized to be SnO (Sn<sup>2+</sup>) and then SnO<sub>2</sub> (Sn<sup>4+</sup>), in which SnO is present at the region closed to interface between Sn-substrate and the tin-oxide layer. At high temperature oxidation, however, Sn was completely oxidized to be SnO<sub>2</sub>.

## 1. Introduction

The presence of lead (Pb) contained in conventional solder material Sn-Pb is known as a hazardous substance that potentially provides effects on the environment and health. Lead poisoning is particularly baneful to the neurological development of children such as damage to the brain, liver and kidney, and hyperactivity effect [1]. Since 2006, therefore, European directives RoHS (restriction of hazardous substances) has declared the regulation to eliminate Pb from the electronic components and devices. This led to the development and execution of Pb-free solders.

Since the last few years Sn-Ag-Cu alloy was considered as one of the most promising lead-free solder alloys for the replacement of conventional solder of Sn-Pb due to its good solderability and relatively high mechanical properties. The Sn-3.0Ag-0.5Cu alloy which is also known as SAC 305 was proposed [2] as one of candidate materials for solder balls grid arrays (BGAs) or solder joints used in electronic packaging (flip-chip packaging) applications. However, Sn-3.0Ag-0.5Cu alloy is easily oxidized after multiple reflows or high aging temperature [3, 4]. The oxygen potential of Sn-oxide formation is actually lower than that of Ag and Cu oxides [5]. This is a key point explaining that Sn is oxidized easily.

Thus, the formation of tin-oxide layer on the surface of solder alloy would inhibit interconnection/bonding between the solder surface and connectors as schematically illustrated in Fig. 1. The growth of tin-oxide



would influence the interface bonding quality. That means when the formation of tin-oxide layer is very thin, good bonding between the two surfaces may be possible [3]. Increase of the thickness of tin-oxide layer will decrease the bond strength.

The oxidation of tin in the solder materials is not a new phenomenon, but studies to overcome the oxidation and wetting problems have been continued until now by adding various alloying elements into the Sn-Ag-Cu alloy such as Sn-Ag-Cu-In [4], Sn-Ag-Cu-Zn [6], Sn-Ag-Cu-Ge [7]. Besides, nanoparticles (nanospherical, nanowires, nanorods) of Pb-free solder alloy of Sn-Ag-Cu have been recently investigated to suppress the melting point of solder material with respect to reduce the oxidation rate of Sn [8-10].

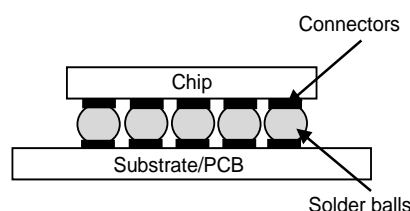


**Figure 1.** Side-view schematic of a typical flip chip

According to various studies on the Sn-Ag-Cu solder alloy especially for solder joint, oxidation of tin is one of significant problems in the interface bonding: i.e. oxidation at room temperature and at reflow/multi-reflow conditions. In this study, the solder balls of Sn-3.0Ag-0.5Cu alloy were oxidized at atmospheric air for about 6 years and, at 85°C and relative-humidity of 85% for 2140 h. Detailed characterization on the tin-oxide formation performed from the cross-section views has not been previously reported. Therefore, morphologies and nanostructure of the oxide nanolayers formed on the surface of Sn-Ag-Cu alloy were studied from the interface between the oxide film and the tin substrate to verify the oxidation mechanism and gain understanding the tin-oxide behavior. This is considered to be important from the viewpoints of both for the fundamental science and industrial applications.

## 2. Experimental methods

Material used in this study was commercial solder balls of Sn-3.0Ag-0.5Cu alloy produced by NIPPON MICROMETAL Co. The solder balls with the diameter of 400  $\mu\text{m}$  or 300  $\mu\text{m}$  were naturally oxidized (at atmospheric air) for about 6 years and at 85°C, relative-humidity of 85% for 2140 h, respectively. They were designated as specimen-1 and specimen-2, respectively. Cross-sectional specimens of the solder ball surfaces were prepared using a focused ion beam (FIB, FB-2000K, Hitachi) equipped with a microsampling unit. Prior to the FIB fabrication, the surface of the solder balls was coated with carbon and tungsten films to prevent the solder ball surface from of  $\text{Ga}^+$  ion bombardment.

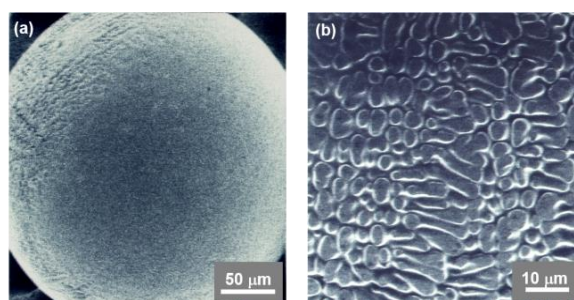


**Figure 2.** SIM image of a solder ball of Sn-3.0Ag-0.5Cu alloy (a) showing the dendritic structure on the surface (b).

Plan-view microstructures of the solder ball surface were observed with FIB-scanning ion microscope (FIB-SIM) as shown in Fig. 2. The dendrite structures covering a solder ball surface may be resulted from solidification during the fabrication process of the solder ball material. Cross-sectional microstructures of the tin-oxide films formed on the solder ball surface were examined by TEM (FEI TECNAI F-20) equipped with scanning TEM (STEM) and the tin-oxide phase was identified by electron diffraction analysis. The areas of tin-oxide layer, interface between the tin-oxide layer and the substrate, and the substrate were also examined

by High resolution TEM (HRTEM) imaging and analyzed by fast Fourier transformation (FFT) to confirm the thickness of the tin-oxide layer and tin-oxide phases, respectively.

### 3. Results and discussion

**Characterization of tin-oxide layer on the solder ball specimen-1.** A cross-sectional bright field (BF)-TEM image of specimen-1 is shown in Fig. 3a. A magnified image of the small rectangular area in Fig. 3a demonstrates a very thin film formed on the substrate with inhomogeneous thickness less than 50 nm (Fig. 3b). The thickness of carbon (C)-coating and tungsten (W)-deposition are also seen. Indexing an electron diffraction pattern (EDP) (Fig. 3A') obtained from a circle area A in Fig. 3a has identified that the thin film was the polycrystalline film consists of SnO and SnO<sub>2</sub>. Diffuse intensity appears in the EDP indicating that some amorphous phases of the tin-oxide are present. An EDP (Fig. B' in (a)) obtained from a circle area B in Fig. 3a confirmed that the substrate was  $\beta$ -Sn.

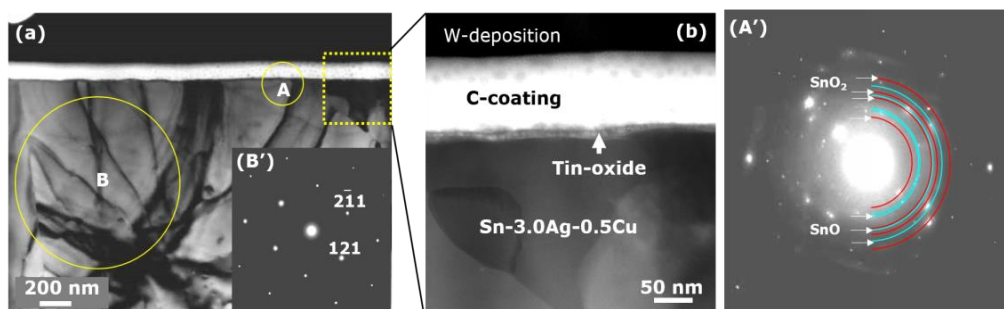


**Figure 3.** (a) A cross-sectional TEM image of specimen-1, (b) a magnified image of a small rectangular area in (Fig. 3a), (A') and (B') are EDPs obtained from circle areas A and B in (a), respectively.

In order to confirm the presence of SnO phase in the oxide nanolayer, an HRTEM image taken from the substrate and the interface between the substrate and the oxide layer is clearly shown in Fig. 4a. The thickness of tin-oxide layer observed in Fig. 4a is around 37 nm.

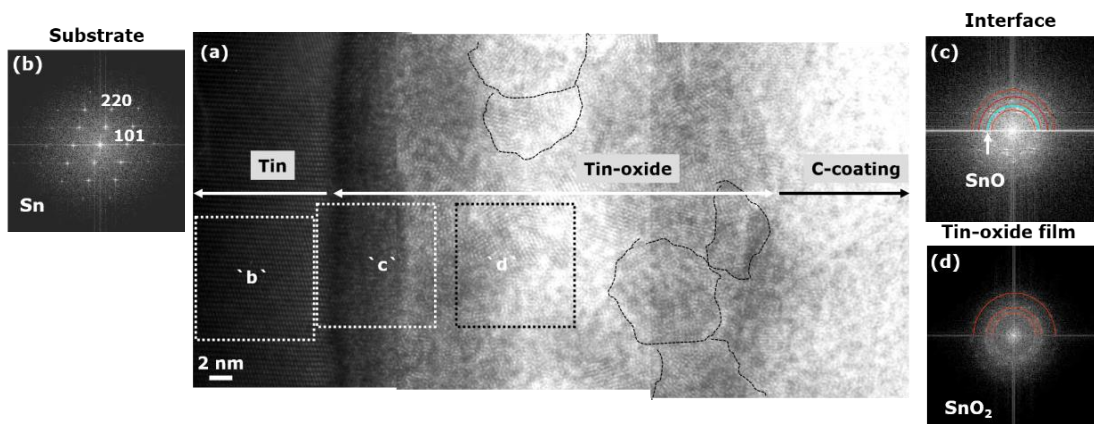


**Figure 4.** (a) A HRTEM image of specimen-1 taken from the area between the tin substrate and carbon coating layer, (b), (c) and (d) Fourier power spectra obtained from areas of the tin substrate ('b'), interface between the substrate and the tin oxide film ('c') and the tin-oxide film ('d'), respectively.

Lattice fringes formed within the tin-oxide layer reveal slightly unclear polycrystalline particle with an average size of about 10 nm. The Fourier power spectra (Fig. 4b, 4c and 4d) related to the areas 'b', 'c' and 'd', respectively have confirmed that SnO is identified at the interface between the substrate and the tin-oxide layer (Fig. 4c). This suggests that SnO is present in the vicinity of the tin substrate surface.

**Characterization of tin-oxide layer on the solder ball specimen-2.** Typical cross-sectional BF-TEM image of solder ball specimen oxidized at 85°C for 2140 h with the incident beam along the [001] zone axis of the tin-substrate (Fig. 5) clearly demonstrated the thin film about 50 nm in thickness (see a white arrow).

Indexing EDPs (Fig. 5b and 5c) obtained from circle areas A and B in Fig. 5a, respectively, indicated that the thin film is made of polycrystalline  $\text{SnO}_2$  formed on the  $\beta$ -tin substrate. No SnO phase was identified.

Based on the entire microstructural observation, thickness of the tin-oxide layer formed on the surface of specimen-2 varies from 40 nm to 50 nm and cracks are developed in some areas of the outer surface of the tin-oxide layer (Fig. 5a). The formation of cracks is not affected by specimen preparation using FIB, but it may be due to stress built-up within the tin-oxide layer. An HRTEM image (Fig. 5d) obtained from the area between the tin-substrate and the carbon-coating layer identified the thickness of tin-oxide layer around 47 nm. Lattice fringes formed in the tin-oxide layer reveal polycrystalline particles in average size ( $\sim 5$ -10 nm) as shown in Fig 4a.

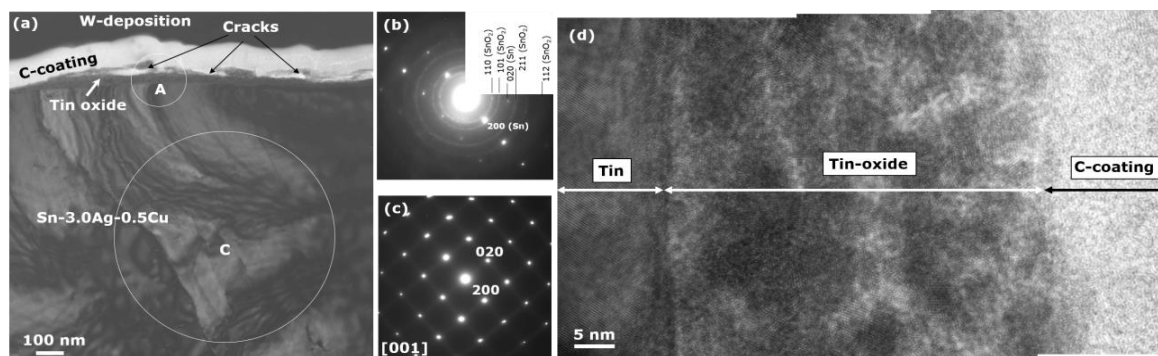


**Figure 5.** (a) A cross-sectional TEM image of specimen-2, (b) and (c) EDPs corresponding to circle areas A and C, respectively, and (d) a HRTEM taken from tin-substrate to carbon layer.

Pure tin and/or tin alloys are very sensitive to oxygen under all conditions even at room temperature because of low oxygen potential of tin ( $\Delta G \sim -110$  Kcal/g.mol  $\text{O}_2$  at 373 K) [5]. When tin is exposed to atmosphere, the oxygen atoms from the atmosphere would diffuse into the tin-surface to form a tin-oxide layer. The formation of non-uniform thickness of tin-oxide layers both on the surface of specimen-1 and specimen-2 is related to the different behavior along the tin-surface. Oxidation of tin nanoparticles at room temperature has indicated that the oxidation rate is particle size-dependence [11]. Combination of XPS and TEM analyzing results have reported that few nanometers ( $\sim 3$  nm) of amorphous SnO layer covered the tin nanoparticles ( $< 100$  nm) surface at room temperature oxidation for about 60 days. This is inconsistent with a result based on Sn nuclear magnetic resonance spectroscopy reported by Kravchyk *et al.* [12] that showed the formation of amorphous  $\text{SnO}_2$  layer covered the colloidal Sn nanocrystals at room temperature oxidation. On the other hand, the tin-oxide thickness of about 3.5 nm formed at the interface between Sn-Ag-Cu bump and the Sn-Ag film after room temperature oxidation for 60 min, but no chemical state of tin-oxide was reported [3].

It is considered that there is a relationship between the chemical state of tin-oxide and the thickness of tin-oxide layer. Polycrystalline SnO and dominantly  $\text{SnO}_2$  are formed within the tin-oxide layer under short-term and long-term room temperature oxidation. Further exposure to air does not change the chemical state of  $\text{Sn}^{2+}$  (SnO) present in the region near the interface between the substrate and the oxide layer, but SnO leads to gradually oxidize to be  $\text{SnO}_2$  in the vicinity toward the surface of the oxide layer exposed to air (gas). It is possible that due to the existence of SnO in the tin-oxide film, the interface bonding strength between tin-oxide film and tin-layer would become weak, and the tin-oxide film would be easily broken.

On the other hand, when oxidation of tin is done at high temperature, Sn would be completely oxidized to be  $\text{SnO}_2$ . No SnO was identified due to SnO is metastable oxide phase. In this case, high temperature accelerates the migration of anion ( $\text{O}^{2-}$ ) across the oxide layer leading higher reaction rate between  $\text{Sn}^{4+}$  and  $\text{O}^{2-}$  to form  $\text{SnO}_2$ .

#### 4. Summary

TEM studies have verified the morphology and nanostructure of tin-oxide nanolayer formed on the tin surface by room and given temperatures oxidation as follows.

- (1) Long-term room temperature oxidation ( $\sim 6$  years) on Sn-3.0Ag-0.5Cu alloy produced inhomogeneous thickness of tin-oxide layer between 20-40 nm. The tin-oxide nanolayer is made of



polycrystalline SnO and predominantly SnO<sub>2</sub> where SnO present in the region near the interface between the substrate and the oxide layer, but SnO leads to gradually oxidize to be SnO<sub>2</sub> in the area toward the surface of the oxide layer.

- (2) Oxidation at 85°C and relative humidity of 85% for 2140 h also produced non-uniform thickness of tin-oxide layer varies between 40-50 nm which is made of polycrystalline SnO<sub>2</sub>. At high temperature oxidation Sn was completely oxidized to be SnO<sub>2</sub>.

### Acknowledgement

This work was supported in part by Nanotechnology Support Project of the Ministry of Education, Culture, Sports, Science and Technology (MEXT), Japan and Research Promotion Bureau, MEXT, Japan.

### References

- [1] Information on <http://www.extraordinaryroadtrip.org/research-library/airpollution/understanding-air-pollution/lead/health.asp>
- [2] Kim K S, Huh S H and Suganuma K 2003 *J. Alloys Compd.* **352** 226
- [3] Wang Y H, Howlader M R, Nishida K, T. Kimura T and Suga T 2015 *Mater. Trans.* **46** 2431
- [4] Lee H and Cho S W 2014 *Appl. Sci. Convergence. Technol.* **23** 345
- [5] Greenwood N N and Earnshaw A 1997 *Chemistry of the Elements*, second ed. Butterworth- Heinemann ISBN 0080379419.
- [6] Zhang L, Han J G, He C W and Guo Y H 2012 *J Mater Sci: Mater Electron* **23** 1950
- [7] Cho S W, Han K, Yi Y, Kang S J, Yoo K H, Jeong K and Whang C N 2006 *Adv. Eng. Mater.* **8** 111
- [8]. Zou C D, Gao Y L, YANG B, Xia X Z, Zhai Q J, Andersson C and Liu J 2009 *J. Electron. Mater.* **38** 351
- [9]. Gao F, Rajathuraia K, Cuia Q, Zhoub G, Acha I N, Z. Gu Z 2012 *Appl. Surf. Sci.* **258** 7507
- [10]. Sun L and Zhang L 2015 *Adv. Mater. Sci. Eng.* **2015** 1
- [11]. Sutter E, Barcelo F I and Sutter P 2014 *Part. Syst. Charact* 1
- [12]. Kravchyk K, Protesescu L, Bodnarchuk M I, Krumeich F, Yarema M, Walter M, Guntlin C and M.V. Kovalenco M V 2013 *J. Am. Chem. Soc.* **135** 4199